Multiscale quantification of tumor microarchitecture for predicting therapy response using dynamic contrast-enhanced ultrasound imaging

Ipek Oezdemir[1], Corinne E. Wessner[2], Collette Shaw[2], John R. Eisenbrey[2], Kenneth Hoyt[1,*]

[1]Department of Bioengineering, University of Texas at Dallas, Richardson, TX, USA
[2]Department of Radiology, Thomas Jefferson University, Philadelphia, PA, USA
* kenneth.hoyt@utdallas.edu

Abstract—**Hepatocellular carcinoma (HCC) is the most common liver cancer with 1 million cases globally. A current clinical challenge is to determine which patients will respond to transarterial chemoembolization (TACE) as effective delivery of the embolic material may be influenced by the tumor vascular supply. The purpose of this study is to develop a novel image processing algorithm for improved quantification of tumor microvascular morphology features using contrast-enhanced ultrasound (CEUS) images and to predict the TACE response based on these biomarkers before treatment. A temporal sequence of CEUS images was corrected from rigid and non-rigid motion artifacts using affine and free form deformation models. Subsequently, a principal component analysis based singular value filter was applied to remove the clutter signal from each frame. A maximum intensity projection was created from high-resolution images. A multiscale vessel enhancement filter was first utilized to enhance the tubular structures as a preprocessing step before segmentation. Morphological image processing methods are used to extract the morphology features, namely, number of vessels (NV) and branching points (NB), vessel-to-tissue ratio (VR), and the mean vessel length (VL), tortuosity (VT), and diameter (VD) from the tumor vascular network. Finally, a support vector machine (SVM) is trained and validated using leave-one-out cross-validation technique. The proposed image analysis strategy was able to predict the patient outcome with 90% accuracy when the SVM was trained with the three features together (NB, NV, VR). Experimental results indicated that morphological features of tumor microvascular networks may be significant predictors for TACE response. Reliable prediction of the TACE therapy response may help provide effective therapy planning.**

Keywords— cancer; hepatocellular carcinoma; transarterial chemoembolization; contrast-enhanced ultrasound; image analysis, microbubble, microvascular networks; machine learning.

I. Introduction

Hepatocellular carcinoma (HCC) is the most common type of liver cancer with 1 million cases globally [1]. Drug-eluting bead transarterial chemoembolization (DEB-TACE or TACE)

procedure is used in patients with unresectable disease stage. Standardized beads size relative to the tumor dimensions are used to deliver chemotherapeutic agents into the tumor angiogenic network via a catheter placed in the tumor-feeding hepatic artery. Following the embolization, the beads start releasing the chemotherapeutic drug slowly into the tumor vasculature. While the occlusion of the tumor vasculature is the indicator of the successful treatment, up to 65-75% of tumors show residual blood flow and in this case repeat TACE or alternative treatments are required [2]. An efficient HCC management would benefit from the information about future TACE response at the time of treatment planning phase. Hence, a current clinical challenge is to determine which patients will respond to TACE as effective delivery of the embolic material may be influenced by the tumor vascular supply.

The morphological features detailing the tumor microarchitecture network may be used as indicators of response to anticancer treatment [3], [4]. To that end, the purpose of the research detailed herein was to investigate the potential of tumor microarchitecture as a pre-therapeutic predictor for TACE therapy response of HCC patients. A novel image processing algorithm for extracting the morphological features of HCC from contrast-enhanced ultrasound (CEUS) images is developed and a support vector machine (SVM) model is trained with a polynomial kernel using different set of the morphological features. Our results suggest that the morphology of the tumor angiogenic network of HCC derived from CEUS images may give pre-therapeutic information about whether a patient is a potential candidate for a TACE complete response. This information may help to provide effective therapy planning strategies and follow-up procedures.

II. Methods

A. Ultrasound Imaging

A retrospective analysis of CEUS images of human HCC was performed ($N = 20$) [5]. All ultrasound (US) examinations were performed using a Logiq E9 scanner equipped with a C1-6-D transducer (GE Healthcare, Wauwatosa, WI). Subjects received a bolus injection of 0.2–0.3 ml of a microbubble (MB) contrast agent (Definity, Lantheus Medical Imaging, N Billerica, MA) followed by a 10 ml saline flush. CEUS imaging

was performed using a dual imaging mode, enabling side-by-side visualization of the grayscale B-mode US and CEUS images at a rate of 8 to 9 frames per sec. A low mechanical index (MI < 0.1) and imaging frequency pairings transmitting at 2 MHz, receiving at the 4 MHz harmonic are used. Patients underwent a pre-therapeutic baseline measurement. Note that post therapeutic magnetic resonance imaging (MRI), computed tomography (CT) and pathology results revealed that 11 subjects were treated successfully while 9 subjects resulted in incomplete response [5].

B. Image Processing

Custom MATLAB (Mathworks, Inc., Natick, MA) software was developed to extract the morphology features. A region-of-interest (ROI) was drawn manually by the sonographer who also conducted the US examinations. The frame with the best visualization of the tumor from the B-mode US image sequence was chosen as the reference frame by a sonographer with over 5 yr experience CEUS. After discarding frames with out-of-plane motion, the affine and non-rigid motion artifacts of CEUS images were corrected using the displacements estimated from B-mode US images [6], [7]. Following that, a singular value filter (SVF) was applied to remove the clutter signal (tissue) from the remaining frames [8]. Finally, a single image is constructed using the maximum intensity projection (MIP) technique. Tubular structures of MIP are enhanced using a multiscale vessel enhancement filter before quantification [9].

C. Morphology Analysis

To use morphological image operations, microvessels from the multiscale image was segmented using an adaptive thresholding method [10]. Once the binary image was created, the morphological features (parameters) were computed using foreground and background pixels, namely, mean number of vessels (NV) and branching points (NB), vessel-to-tissue ratio (VR), and mean vessel length (VL), tortuosity (VT) and diameter (VD) [11].

Morphological parameters from tumor microarchitecture were then used to train different machine learning models to evaluate the predictability of future therapy response as a classification task in two classes, i.e. complete and incomplete response. SVM models using a linear, polynomial, and radial kernels were trained and validated [12]. Data were centered and scaled in a preprocessing step before training. The leave one out cross-validation method was used to avoid the overfitting due to the limited sample size. The polynomial kernel was chosen as it was the simplest and the best performing model. For a better model assessment, three different models were trained with the same hyper-parameter settings using a single feature (NV), a set of features (NV, NB, VR), and finally all of the features (NV, NB, VR, VL, VT, VD). The three SVMs were compared in terms of accuracy and interrater reliability (kappa). The generalization of the model was measured by the number of the support vectors. Statistical analyses were implemented using the R Project for Statistical Computing [13].

III. RESULTS AND DISCUSSION

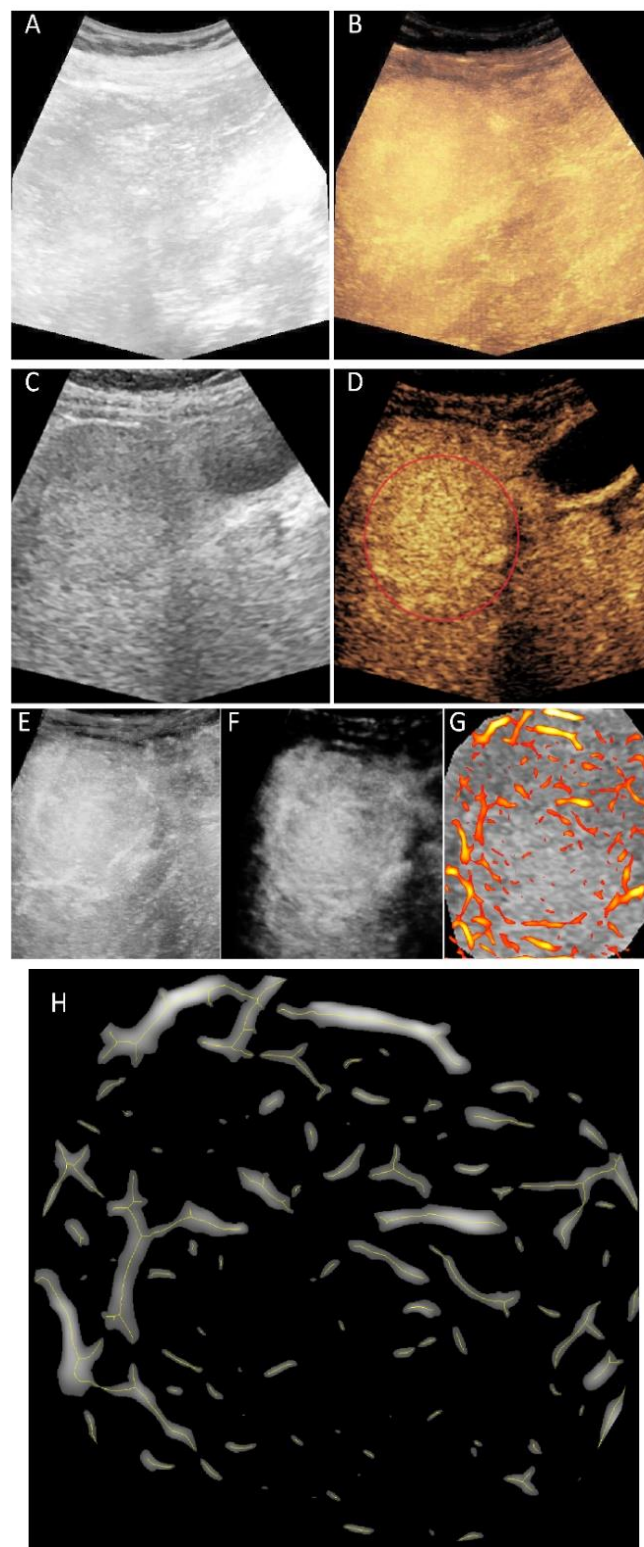The use of morphological features as tumor response predictors was evaluated in 20 patients who received HCC

Fig. 1. Representative outcome from image processing steps. The maximum intensity projection (MIP) images from original B-mode ultrasound (US) (A) and contrast-enhanced US (CEUS) (B) image sequences. Region-of-interest (ROI) selection from a single B-mode US (C) and CEUS (D) image. Motion corrected version of the CEUS-MIP (E) and the result of clutter filtering (F). Enhanced tubular structures overlaid on original and resized B-mode US reference for only the tumor region (G). Centerlines of the vessel on enlarged tumor area used for morphological feature extraction (H).

TACE therapy. According to the CT, MRI and pathology outcomes, 11 patients had complete response and the other 9 had incomplete response. Figure 1 illustrates representative results from the image processing pipeline. The original MIP from B-mode US (A) and CEUS (B) images provide an example where the tumor visualization was challenging. In (C) and (D) the reference images used for motion correction and ROI selection are depicted. The image in (E) is the result after motion correction was applied and (F) is the outcome from clutter filtering. The enhanced tubular structures processed with morphological spatial filters are overlaid on the original B-mode US MIP (G). Finally, the simplified angiogenic network (skeleton) is overlaid on the tumor microarchitecture in (H).

The results from the model comparison using three different feature sets are listed in Table I. Comparing three models with increasing number of features allowed us to have a better control on potential model overfitting. SVM achieved 80 % accuracy with 10 support vectors (SV) and 0.2 training error when using only one feature (NV). Training on the features (NB, NV, and VR), improved the accuracy to 90 % obtained with 4 SVs and 90 % accuracy was achieved with 6 SVs when the data was trained in a six dimensional feature space (NB, NV, VR, VL, VT, and VD). Latter two models with three and six features were able to complete the training with a zero training error and having small amount of support vectors is an indicator that the models were generalizable. For this amount of data, the second model trained with NB, NV, and VR was found to be the best performing model.

Complex tumor microvascular network may affect the arterial delivery of the drug-eluting beads into the tumor vasculature during TACE. If it is believed the intra-arterial therapies will not provide adequate treatment response, alternative locoregional therapies such as ablation of radiation maybe employed. In this current study, the preliminary results demonstrated that less complex tumors have a higher potential for a complete response to TACE therapy. This may be partially attributed to the fact that more developed tumor vasculature may develop multiple feeding sources, requiring multiple TACE treatments for complete embolization. Thus, results exhibited that pre-therapeutic morphological features of tumor microvascular networks can help decide what patients are good candidates for a successful TACE treatment and what patients may benefit less.

Previous studies have shown that preoperative conventional MRI features and texture analysis can predict high-risk of non-complete response of TACE + high-intensity focused US (HIFU) treatment [14]. Also the texture features from CT images were shown to be potential predictors for identifying patients who are not suitable for TACE treatment [15]. Considering the high cost of cross sectional imaging, concerns surrounding the nephrotoxicity of CT and MRI contrast, as well as the ionizing properties of CT imaging modalities, a reliable prediction using CEUS-derived features may be the preferred method.

Since tumor morphology exists inherently in three-dimensional (3D) space, development of 3D CEUS methods [16]–[18] are necessary for improved quantification of the

TABLE I. PERFORMANCE METRICS FOR SELECT FEATURES

Trained Features	Accuracy	Kappa (#SV)
NV	80 %	59 % (10)
NV,NB,VR	90 %	79 % (4)
NV,NB,VR,VL,VT,VD	90 %	79 % (6)

#SV=Number of support vectors

morphological features from HCC microarchitecture. Hence, future work will include more patients and the development of 3D image processing algorithms to perform the same analysis using a volumetric approach.

IV. CONCLUSION

Preliminary results demonstrated that morphological features of tumor microvascular networks may be significant predictors for TACE response. Reliable prediction of the TACE therapy response may help to provide effective therapy planning strategies.

REFERENCES

[1] E. P. Weledji, G. Enow Orock, M. N. Ngowe, and D. S. Nsagha, "How grim is hepatocellular carcinoma?" *Annals of Medicine and Surgery*, vol. 3, no. 3, pp. 71–76, 2014.

[2] C. M. Shaw *et al.*, "Contrast-Enhanced Ultrasound Evaluation of Residual Blood Flow to Hepatocellular Carcinoma After Treatment With Transarterial Chemoembolization Using Drug-Eluting Beads," *Journal of Ultrasound in Medicine*, vol. 34, no. 5, pp. 859–867, 2015.

[3] K. Hoyt, H. Umphrey, M. Lockhart, M. Robbin, and A. Forero-Torres, "Ultrasound imaging of breast tumor perfusion and neovascular morphology," *Ultrasound Med Biol*, vol. 41, no. 9, pp. 2292–2302, 2015.

[4] R. Saini and K. Hoyt, "Recent developments in dynamic contrast-enhanced ultrasound imaging of tumor angiogenesis," *Imaging Med*, vol. 6, no. 1, pp. 41–52, 2014.

[5] K. Nam *et al.*, "Evaluation of hepatocellular carcinoma transarterial chemoembolization using quantitative analysis of 2D and 3D real-time contrast enhanced ultrasound," *Biomedical Physics & Engineering Express*, vol. 4, no. 3, p. 035039, 2018.

[6] I. Oezdemir, C. Shaw, J. R. Eisenbrey, and K. Hoyt, "Improved quantitative contrast-enhanced ultrasound imaging of hepatocellular carcinoma response to transarterial chemoembolization," *IEEE International Symposium on Biomedical Imaging*, 1737-1740, 2019.

[7] S. Harput *et al.*, "Two-stage motion correction for super-resolution ultrasound imaging in human lower limb," *IEEE Transactions on Ultrasonics, Ferroelectrics, and Frequency Control*, vol. 65, no. 5, pp. 803–814, 2018.

[8] F. W. Mauldin, D. Lin, and J. A. Hossack, "The singular value filter: A general filter design strategy for PCA-based signal separation in medical ultrasound imaging," *IEEE Transactions on Medical Imaging*, vol. 30, no. 11, pp. 1951–1964, 2011.

[9] A. F. Frangi, W. J. Niessen, K. L. Vincken, and M. A. Viergever, "Multiscale vessel enhancement filtering," in *SpringerLink*, 1998, pp. 130–137.

[10] D. Bradley and G. Roth, "Adaptive thresholding using the integral image," *ACM J. Graph. Tools*, pp. 13–21, 2007.

[11] I. Özdemir and K. Hoyt, "Morphological processing for multiscale analysis of super-resolution ultrasound images of tissue microvascular networks," in *Medical Imaging 2019: Ultrasonic Imaging and Tomography*, vol. 10955, p. 1095505, 2019.

[12] C. Cortes and V. Vapnik, "Support-vector networks," *Mach Learn*, vol. 20, no. 3, pp. 273–297, 1995.

[13] "R: The R Project for Statistical Computing." Available: https://www.r-project.org.

[14] J. Y. Yu *et al.*, "Value of texture analysis based on enhanced MRI for predicting an early therapeutic response to transcatheter arterial chemoembolisation combined with high-intensity focused ultrasound treatment in hepatocellular carcinoma," *Clinical Radiology*, vol. 73, no. 8, pp. 758.e9-758.e18, 2018.

[15] H. J. Park *et al.*, "Prediction of therapeutic response of hepatocellular carcinoma to transcatheter arterial chemoembolization based on pretherapeutic dynamic CT and textural findings," *American Journal of Roentgenology*, vol. 209, no. 4, pp. W211–W220, 2017.

[16] K. Hoyt, A. Sorace, and R. Saini, "Quantitative mapping of tumor vascularity using volumetric contrast enhanced ultrasound," *Invest Radiol*, vol. 47, no. 3, pp. 167–174, M2012.

[17] M. Mahoney, A. Sorace, J. Warram, S. Samuel, and K. Hoyt, "Volumetric contrast-enhanced ultrasound imaging of renal perfusion," *J Ultrasound Med*, vol. 33, no. 8, pp. 1427–1437, 2014.

[18] K. Hoyt, A. Sorace, and R. Saini, "Volumetric contrast-enhanced ultrasound imaging to assess early response to apoptosis-inducing anti-death receptor 5 antibody therapy in a breast cancer animal model," *J Ultrasound Med*, vol. 31, no. 11, pp. 1759–1766, 2012.